High-Fidelity CFD Modeling of Maneuvering Projectile Aerodynamics

Jubaraj Sahu, Sidra Silton, and Karen R. Heavey
U.S. Army Research Laboratory
Aberdeen Proving Ground, Maryland 21005
Jubaraj.sahu.civ@mail.mil

ABSTRACT

This paper describes the recent progress made in the design and development of a highly-maneuverable canard-controlled projectile capable of engaging moving targets. Numerical computations have been performed using Navier-Stokes computational fluid dynamics (CFD) techniques for a number of projectile configurations primarily focused on the aft section of the projectile. Results from these computations are combined in an optimization routine. In addition, a canard-controlled highly-maneuverable configuration has been used to study the effect of canard deflection angle on the aerodynamics and flight dynamics of this projectile for roll control maneuver. Currently, work is in progress and coupled CFD/rigid-body dynamics (RBD)/flight control system (FCS) techniques are being employed for this projectile. Computed results from this effort will be compared with limited roll control data available from a wind tunnel test. Design of an optimized highly-maneuverable canard-controlled projectile continues with both uncoupled and coupled methods.

1. INTRODUCTION

Understanding the aerodynamics of projectiles, rockets, and missiles is critical to the design of stable configurations and contributes significantly to the overall performance of weapons systems. The prediction of aerodynamic coefficients for these weapons systems is essential in assessing the performance of new designs.[1,2] Numerical simulations have the potential of greatly reducing design costs, while providing a detailed understanding of the complex aerodynamics associated with each change. This is especially true of maneuvering munitions. Airframe designs that offer high-maneuverability are required to engage moving targets.

Generally, maneuvering munitions require the use of complex control surfaces (fins and canards), control mechanisms, and/or the use of flow technologies such as micro-jet gas generators to provide maneuver authority. The aerodynamic flow fields over these maneuvering munitions are complex, involving non-linear flow-physics, especially during and after control maneuvers because of flow interactions. For maneuvering munitions, however, very limited data is available during and after control maneuvers, and there is a lack of knowledge and understanding of the associated unsteady aerodynamics and flow interactions. [3,4] This continues to be a significant issue during the design process of maneuvering munitions. Accurate numerical modeling of the unsteady aerodynamics and flow interaction effects has been found to be challenging, both in terms of time-accurate solution techniques and computing resources required. Improved computer technology and state-of-the-art uncoupled computational fluid dynamics (CFD) procedures now allow solutions to be obtained in a timely manner for standard projectile design. For design of maneuvering munitions, it is still a difficult endeavor. As part of a DoD Grand Challenge Project, we continue to focus on the development and application of advanced time-accurate CFD and coupled CFD/rigid-body dynamics (RBD)/flight control system (FCS) techniques for prediction of the unsteady free-flight aerodynamics and flight behavior of maneuvering projectiles in actual flights.[5,6]

In the present effort, advanced CFD techniques are being exploited on modern HPC machines to provide the accurate determination of aerodynamic performance required for design and analysis of a highly-maneuverable munitions configuration. For the first part, various body-fin configurations were considered with special emphasis on the aft-end of the projectile. For these initial configurations, a comprehensive grid resolution and turbulence model study was completed. The computational aerodynamic coefficients for the body-fin configurations were integrated with previously determined canard aerodynamic coefficients for use in an aerodynamic optimization routine. The second part deals with the assessment of canard-control aerodynamics and validation of the coupled CFD/RBD/FCS[6] using a canard-controlled body-fin configuration. Although not optimized for performance, this canted fin-stabilized, canard-controlled projectile was chosen since limited roll control wind tunnel data is available for validation of the coupled CFD/RBD/FCS method. Once validated, the coupled method, which takes into account all the unsteady aerodynamics and flow interaction effects in an integrated manner, can lead to improved FCS and highly-maneuverable designs.

This paper describes the recent progress made in the design and development of a highly-maneuverable munition using advanced CFD techniques. The following sections describe the numerical solution techniques and the computed results obtained for initial designs/configurations.

2. COMPUTATIONAL METHODOLOGY

The complete set of three-dimensional (3-D) time-dependent Reynolds-Averaged Navier-Stokes (RANS) equations is solved using the finite-volume method[7]:

$$\frac{\partial}{\partial t}\int_V \boldsymbol{W}\, dV + \oint [\boldsymbol{F} - \boldsymbol{G}] \cdot dA = \int_V \boldsymbol{H} dV$$

where **W** is the vector of conservative variables, **F** and **G** are the inviscid and viscous flux vectors, respectively, **H** is the vector of source terms, V is the cell volume, and A is the surface area of the cell face. Second-order discretization was used for the flow variables and the turbulent viscosity equations. Two-equation *k*-ε and three-equation *k*-*ε*-*R* turbulence models were used for the computation of turbulent flows.[8]

Also of interest is the digital virtual aerodynamic range technique using coupled CFD/RBD/FCS procedure. The coupled procedure uses the same CFD capability and solves the unsteady Navier-Stokes equations, above. In addition, it incorporates unsteady boundary conditions and a special coupling procedure. It allows "virtual fly-out" of projectiles on the supercomputers, and it predicts the actual fight paths of a projectile and all the associated unsteady free-flight aerodynamics using coupled CFD/RBD/FCS techniques in an integrated manner. In the coupled CFD/RBD procedure, the forces and moments are computed every CFD time-step and transferred to a six-degrees-of-freedom (6-DOF) module which computes the body's response to the forces and moments. In the fully-coupled CFD/RBD/FCS mode, control of a projectile can be achieved in many different ways, e.g., with canards and pulse jets during the flight. The control system strategy is conveyed through a control law. The output of RBD state and the control variables are transferred to the CFD flow solver. For example, for a canard-controlled projectile, the output of the FCS variables would be the canard deflection angles. As canards are moved to the FCS-generated deflection angles, the flow solver must take into account the canard motion.

3. RESULTS

Results obtained using advanced CFD techniques are presented first, for the CFD-based design study, and second for a canard-controlled finned projectile.

3.1. CFD-Based Development of a High-Maneuverability Munition

An effort was undertaken to begin development of a high-maneuverability airframe for use in the engagement of moving targets. To this end, a computational analysis to determine the aerodynamic coefficients was completed for possible body-fin configuration with particular emphasis on the aft-end of the projectile. A comprehensive grid resolution, turbulence model, and computational code version study was completed on the initial configuration, but is not included here for brevity. In this phase of the work, the computational aerodynamic coefficients for the body-fin configurations were integrated with previously determined canard aerodynamic coefficients for use in an aerodynamic optimization routine.

Several body-tail configurations were investigated during the course of this study. The fore-body was kept constant with a body reference diameter of 83 mm, as was the nose; the fin blade span (i.e., the distance from the body to the fin tip), fin axial position from the base of the projectile, and the center-of-gravity location 200 mm

from the nose. There were three basic configurations and up to five variations of each configuration. The three basic configurations consisted of the baseline shoulder-launched configuration (Fig 1a), an artillery aft-end (Fig. 1b), and a mortar aft-end (Fig 1c). Variations including overall length, exclusion of boom, and internal boom were also considered, but results are not included here, again for brevity. Figure 2 shows a computational mesh near the projectile. Cylindrical density boxes were placed in the wake of the projectile and around the fins to ensure proper grid resolution in these areas. The resulting meshes were contained to 14-18 million cells, depending on configuration and the first-specified prism layer spacing.

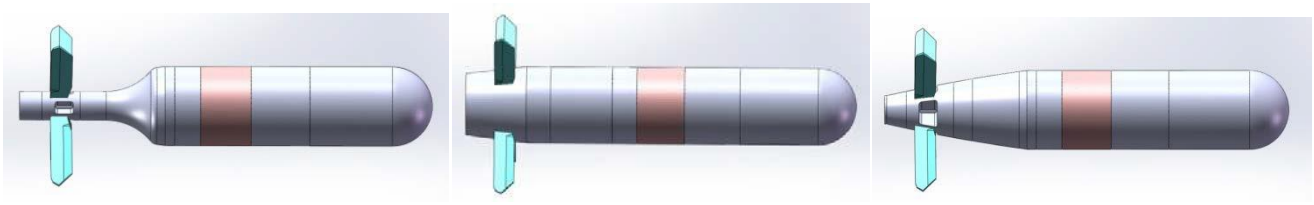

(a) (b) (c)

Figure 1. Three baseline configurations investigated. (a) baseline shoulder-launched, (b) artillery aft-end, (c) mortar aft-end.

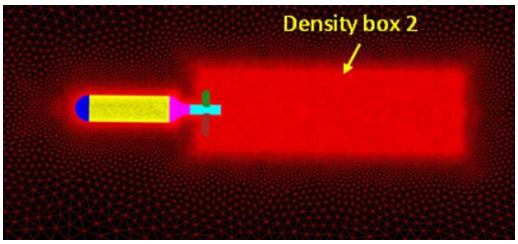

Figure 2. Close-up of mesh near the projectile showing locations of density boxes.

The static aerodynamic characterization of the baseline shoulder-launched munition (C01_V01) was completed using a mesh with boundary-layer spacing for solve-to-wall integration on fins and wall functions elsewhere, and the k-ε-R turbulence closure model. Many angle-of-attack simulations were completed for each of the three Mach numbers (Mach 0.5, 0.65, 0.8), for a total of 21 simulations. Each simulation was run for many thousands of iterations to ensure convergence in both residual drop as well as aerodynamic coefficients. The aerodynamic coefficients were then obtained by averaging their values over the last 200 iterations to minimize any oscillations (mostly present at higher angles-of-attack). After determining that the baseline shoulder-launched munition would not meet static stability requirements for a non-rolling, canard-maneuvered airframe, it was desired to investigate the effect that modifications to the aft-end of the projectile would have on performance. Once again, the aerodynamic investigation would take place on the body-fin configuration only. Specifically, it was desired to know how changes to the aft-end only (fin blade span stayed constant) would affect stability, range and maneuverability. To this end, two additional aft-end configurations (artillery (C02) and mortar (C03)) were investigated, along with multiple variations of each.

Computed normal force and pitching moment coefficients for the three configurations are shown in Figure 3. The artillery configuration has significantly more body lift, resulting in a greater total normal force for a given angle-of-attack than the other two configurations (Fig.3a). The variation in C_m (Fig.3b) between configurations can be attributed to the tip-to-tip span of the fins and the percentage of the fin blade that remains in the shadow of the body flow. Figure 4 shows the lower pressure that occurs on the fins blades of the artillery base as it is exposed to the flow. This lower pressure on the leeward side of the fins on artillery shaped round causes a more negative pitching moment and, hence, a more stable round. As the flow around the fins on the mortar aft-end shape is similar to that of the shoulder-launched munition, the fin effectiveness is similar as well. The benefit of the mortar shape over the shoulder-launched munition appears to be the elimination of the recirculation

region between the boat-tail and the boom. Unfortunately, the stability of this baseline mortar shape (C03_V01) is no better than that of the original shoulder-launched munition (C01_V01), and at larger angles-of-attack is actually worse. However, the artillery aft-end (C02_V01) shows promise with a significantly greater static margin. The findings at the higher two Mach numbers were similar.

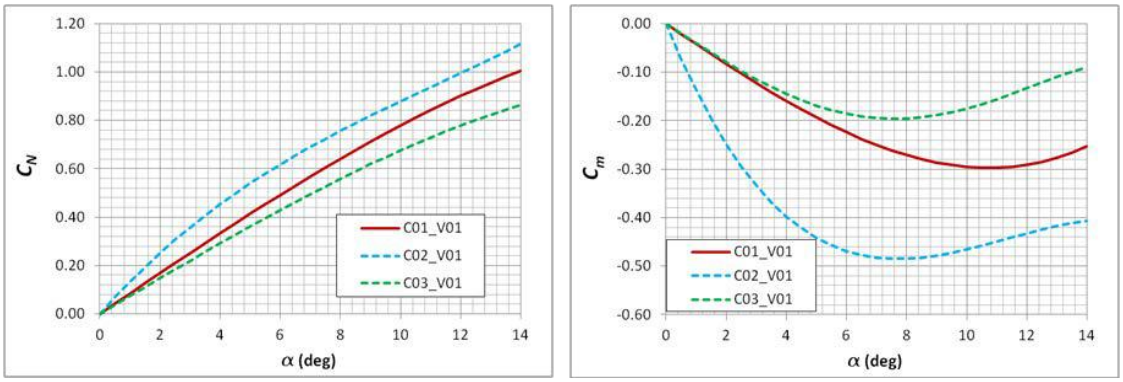

Figure 3. Comparison of aerodynamic coefficients of each aft-end configuration, version 1at Mach 0.5.

Analysis of the optimal airframe suggests an artillery aft-end with proper selection of fins and canards may provide the best maneuverability. However, the optimal parameters produced a very flat pitching moment curve indicating a sensitive design. Physical constraints of the airframe space claims will likely limit the size and placement of the canards. In the results presented so far, the flow interactions were not properly modeled in the current super-position of canard and body-fin aerodynamic data. A more advanced analysis that takes into account all flow interaction effects is currently being conducted.

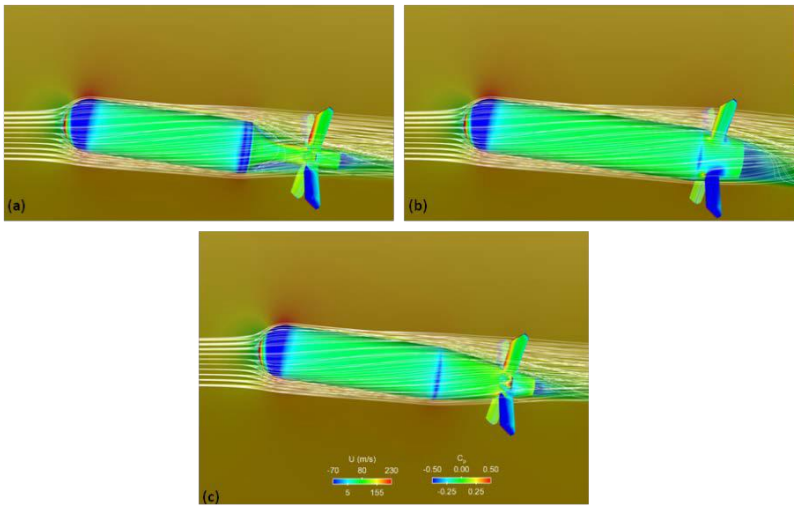

Figure 4. Centerline velocity contours, surface pressure coefficients, and streamlines at Mach 0.5, α = 8° for (a) C01_V01, (b) C02_V01, and (c) C03_V01.

3.2. Canard Maneuvers for a Canard-Controlled Projectile in Subsonic Flight

For assessment of canard-control aerodynamics and validation of the coupled CFD/RBD/FCS code, a different configuration, shown in Figure 5, was considered. Although not optimized for performance, this canted fin-stabilized, canard-controlled projectile was chosen since some wind tunnel data on roll control is available for validation of coupled CFD/RBD/FCS method. Of interest here is the control of the projectile using four canards located in the nose section of the projectile. These canards are used to provide the control forces needed to maneuver a projectile. The canards are deflected to generate control forces required to maneuver the projectile in roll, pitch, or a combination of both. The resulting flow fields involve flow interactions on the projectile body, including the rear fins, and must be taken into account in the CFD simulations. A structured grid is generated on (and around) one canard first, and then the same canard mesh is rotated and used for the other three canards. The four canard grids are then overset with the background projectile mesh generated separately to form a Chimera overlapped mesh for the canard-controlled projectile (see Fig. 6). The total number of grid

points in this case is approximately 30 million. This Chimera procedure has been used previously[9] and requires proper transfer of information between the background mesh and the canard meshes. However, the advantage of a Chimera overlapped mesh is that the individual grids are generated only once, and the Chimera procedure can then be applied repeatedly as required during the canard motion. There is no need to generate meshes at each time-step during the canard deflections/maneuvers.

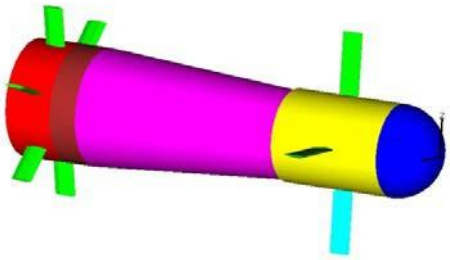

Figure 5. Canard-controlled projectile configuration.

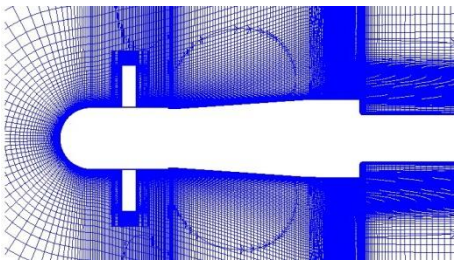

Figure 6. Expanded view of grid near the projectile.

Numerical computations have been performed for this projectile at Mach 0.5 for various angles-of-attack, roll orientations, and canard-deflection angles. Representative qualitative features of the canard-control interaction flow fields are shown in Figure 7 at α = 0° and 5°. This figure shows the computed pressure contours on the surface of the projectile at a given roll orientation of 22.5° for three different canard-deflection angles. As the canards are deflected, the surface pressures change over the length of the body and especially near the canards and the rear fins. The flow from the nose to the base of the body is asymmetric as expected at an angle-of-attack, α = 5°.

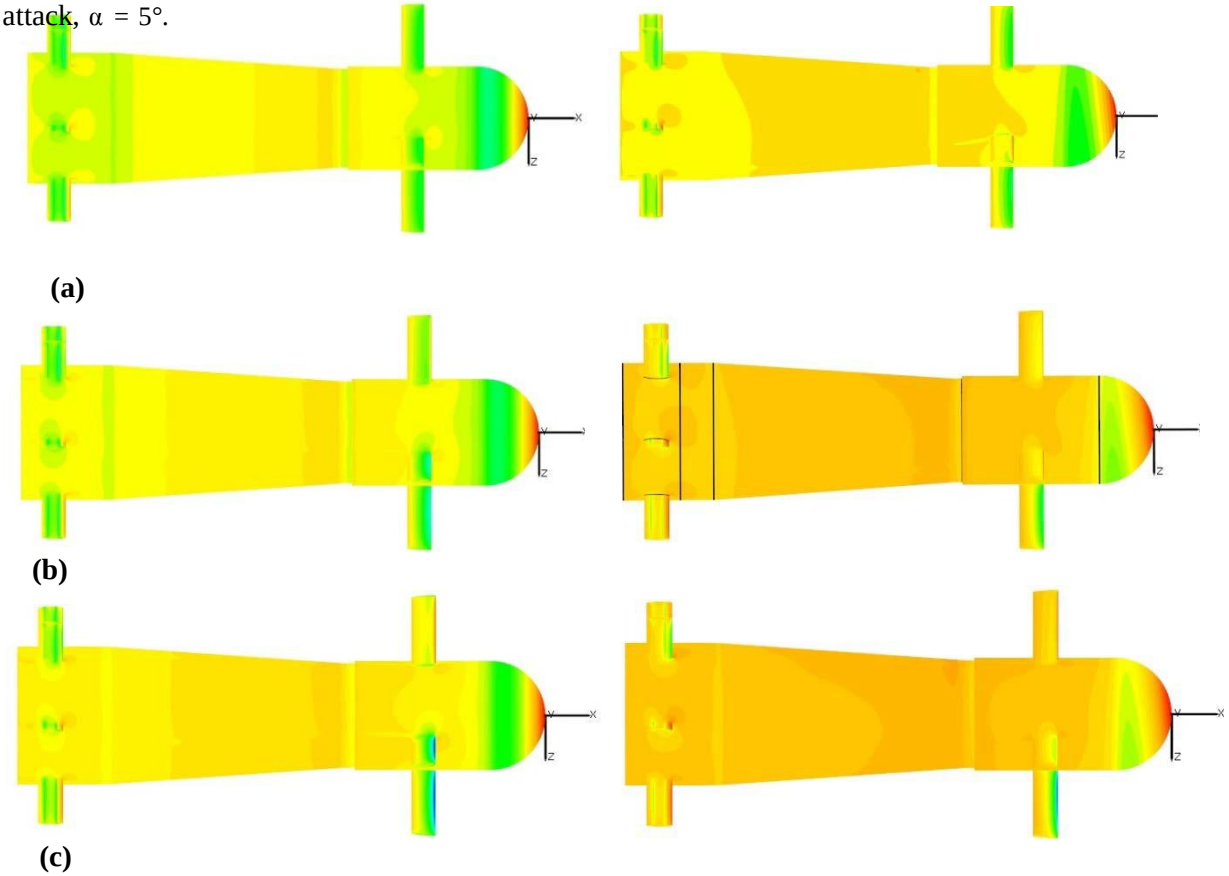

Figure 7. Computed surface contours at M ach= 0.5, α = 0° (left), and α = 5° (right) for different canard deflections, (a) 0°, (b) 4°, (c) 8°.

The effect of the canard-deflections on the roll moment of the projectile is shown in Figure 8. With increase in the canard-deflection angle, the roll moment coefficient is increased (becomes more negative). As seen in this figure, the effect of roll orientations from zero to 22.5° is a very negligible at $\alpha = 0°$ and only small differences can be observed at an angle-of-attack, $\alpha = 5°$.

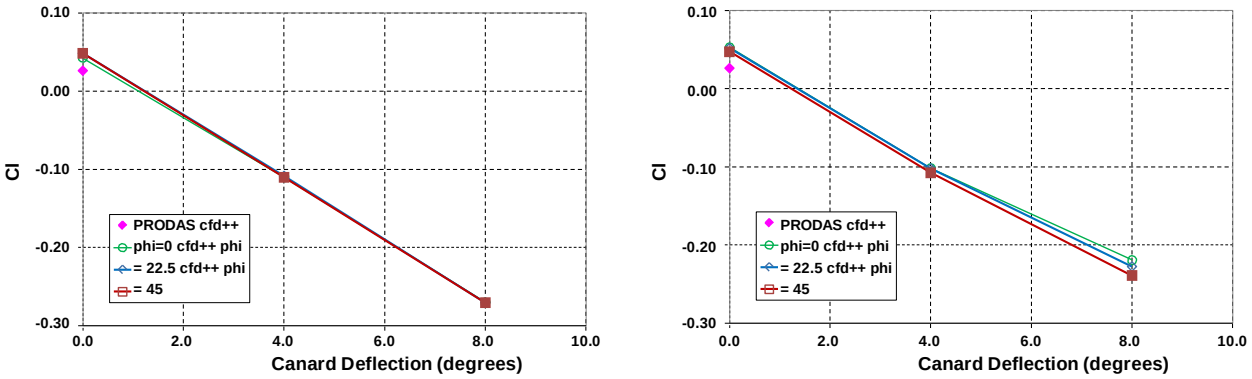

Figure 8. Effect of canard-deflection on rolling moment, Mach = 0.5at $\alpha = 0°$ (left) and $\alpha = 5°$ (right).

Currently, work is in progress on the coupled CFD/RBD/FCS simulations, which are being performed to further investigate the canard-fin flow interaction effects, including whether they differ between static and dynamic, coupled and uncoupled simulations, for this canard-controlled projectile. Results obtained from the coupled simulations will be compared with available roll control wind tunnel test data. Validated coupled CFD/RBD/FCS technique along with uncoupled CFD and 6-DOF simulations can be used for physics-based design of canard-control projectiles for optimized performance.

4. CONCLUDING REMARKS

This paper describes recent progress made towards the design and development of a highly-maneuverable projectile using canard control. Advanced CFD techniques are being utilized, along with an optimization routine for design and analysis of various configurations. All CFD computations were performed on highly-parallel IBM and SGI Clusters at the ARL and AFRL DSRCs using an advanced, scalable, unstructured flow solver. Computed results have provided some insight into the after-body flow fields and improved after-body designs. More research is planned to determine how to most efficiently and fully account for the canard-fin interactions and unsteady flow effects in the design and analysis process. In an effort to begin to address these flow interaction issues, a canard-controlled highly-maneuverable configuration has been used to study the effect of canard deflection angle on the aerodynamics of this projectile for a roll control maneuver. Computed results obtained using uncoupled CFD method show the effect of canard-deflection angles and roll orientations. Currently, work is in progress to investigate canard flow interaction effects using the coupled method and roll control maneuvers. As there is roll control wind tunnel data available for this canard-controlled projectile configuration, validation of coupled CFD/RBD/FCS method for a canard-controlled maneuver will be possible. Further development of the coupled method will extend its capability to guided trajectory control with pulse jets and other control mechanisms. These research efforts will provide accurate unsteady aerodynamics and flight dynamics predictions, which inherently include the flow interaction effects associated with guided maneuvers. This will ultimately lead to increased maneuverability for the next-generation, low-cost munitions required to hit moving targets.

Acknowledgments

The authors would like to thank the Department of Defense High Performance Computing Modernization Program Office for sponsoring this work as a part of a Grand Challenge Project and for providing critically needed HPC resources at ARL DSRC and AFRL DSRC for successful accomplishment of the work.

References

1. Silton, S., "Navier-Stokes Computations for a Spinning Projectile from Subsonic to Supersonic Speeds," *Journal of Spacecraft and Rockets*, Vol 42, No 2, pp. 223-231, 2005.
2. DeSpirito, J., and Plostins, P., "CFD Prediction of M910 Projectile Aerodynamics: Unsteady Wake Effect on Magnus Moment," AIAA-2007-6580, Aug. 2007.
3. Sahu and Heavey, K.R, "Unsteady CFD Modeling of Micro-Adaptive Flow Control for an Axisymmetric Body", *International Journal of Computational Fluid Dynamics*, Vol. 5, April-May 2006.
4. Costello, M., "Extended Range of a Gun Launched Smart Projectile Using Controllable Canards," *Shock and Vibration*, Vol 8, No 3-4, pp. 203-213, 2001.
5. Sahu, J., "Time-Accurate Numerical Prediction of Free-Flight Aerodynamics of a Finned Projectile," *AIAA Journal of Spacecraft and Rockets*, Volume 45, Number 5, Sep/Oct 2008.
6. Sahu, J., Costello M., and Montalvo, C., "Development and Application of Multidisciplinary Coupled Computational Techniques for Projectile Aerodynamics" *7th International Conference on Computational Fluid Dynamics*, Kohala Coast, HI, Jun 2012.
7. Peroomian, O. and Chakravarthy S., "A `Grid-Transparent' Methodology for CFD," AIAA Paper 97-0724, Jan. 1997.
8. U. Goldberg, O. Peroomian, and S. Chakravarthy, "A Wall-Distance-Free K-E Model with Enhanced Near-Wall Treatment" *ASME Journal of Fluids Engineering*, Vol. 120, 457-462, 1998.
9. J. Sahu and C. J. Nietubicz, "Application of Chimera Technique to Projectiles in Relative Motion", *Journal of Spacecraft & Rockets*, Sept-Oct 1995.